Biosensors and Bioelectronics 127 (2019) 25–30

Contents lists available at ScienceDirect

Biosensors and Bioelectronics

journal homepage: www.elsevier.com/locate/bios

# Hexaammineruthenium (II)/(III) as alternative redox-probe to Hexacyanoferrat (II)/(III) for stable impedimetric biosensing with gold electrodes

Julian D. Schrattenecker[a,*], Rudolf Heer[a], Eva Melnik[a], Thomas Maier[a], Günter Fafilek[b], Rainer Hainberger[a]

[a] AIT Austrian Institute of Technology GmbH, 1210 Vienna, Austria
[b] Institute of Chemical Technologies and Analytics, Technische Universität Wien, 1060 Vienna, Austria

ARTICLE INFO

*Keywords:*
Electrochemical biosensor
Gold electrode, Hexacyanoferrat (II)/(III)
Hexaammineruthenium (II)/(III)
Electrochemical impedance spectroscopy
IgG

ABSTRACT

Gold electrodes have been used in a wide range of electrochemical biosensors because their functionalization process with thiols has been well described and, in general, they offer good chemical stability. However, one of the most commonly used redox-pairs in electrochemical impedance spectroscopy, Hexacyanoferrate (II)/(III), causes corrosion of the gold electrodes and consequently damages the surface modification. This leads to alterations of the sensing signals, and thus, renders the quantitative and sensitive detection of target molecules virtually impossible. To overcome this problem we introduced the in-situ generation of Hexaammineruthenium (II)/(III) as redox-pair during the impedimetric measurement by applying a DC-bias. This DC-bias was chosen in such a way that it supplied Hexaammineruthenium (II) in a suitable concentration at the electrode surface by reducing Hexaammineruthenium (III). We compared the stability of photolithographically fabricated thin-film and screen-printed gold electrodes in Hexacyanoferrate and Hexaammineruthenium solutions. Further, long-time characterization of the electrochemical properties with cyclic voltammetry and electrochemical impedance spectroscopy revealed that Hexaammineruthenium (II)/(III) was an excellent redox-pair for stable impedimetric measurements with gold electrodes. To demonstrate the suitability of Hexaammineruthenium for biosensing we applied it for the impedimetric detection of human-IgG. This biosensor exhibited a linear range from 11.3 ng/mL to 113 µg/mL, which is a suitable range for diagnostic applications.

## 1. Introduction

Electrochemical biosensors have been studied intensively during recent years (El Harrad et al., 2018; Huang et al., 2017; Moon et al., 2018). Not only the variety of measureable biomarkers has increased tremendously, also the optimization has been a focus of research to improve the limit of detection and the linear range. In particular, electrochemical biosensors based on electrochemical impedance spectroscopy (EIS) have attracted much interest because they can provide a sensitive label-free transducer platform, which is highly appealing for point-of-care diagnostic applications (Bahadır and Sezgintürk, 2016; Mills et al., 2018; Randviir and Banks, 2013). For the detection of biomarkers, surface modifications with antibodies are commonly chosen because of the huge variety of target molecule matches and their dominating role in enzyme linked immunosorbent assay (ELISA) or microarray test systems. In contrast to the established analytical methods, the EIS biosensing principle allows surface sensitive detection of target molecules in the lower ng/mL ranges without using a label. In faradaic EIS a redox-pair is available in the solution and by applying a sinusoidal voltage with a small amplitude over a broad frequency range, typically from 0.1 Hz to 1 MHz, the charge transfer resistance ($R_{CT}$), the double-layer capacitance ($C_{DL}$), the solution resistance ($R_S$) and the Warburg impedance ($Z_W$) of a Randles-type equivalent circuit can be determined (Bănică, 2012). To produce a working EIS biosensor, receptor molecules have to be immobilized on the surface, so they can specifically bind the target molecules from the solution by antibody-antigen interaction. The bound analyte molecules on the surface increase the $R_{CT}$ in correlation with the concentration in solution. This enables the detection of very differently sized molecules from small sizes such as hormones (Arya et al., 2010) up to very large molecules such as Immunoglobulin G (IgG) (Montes et al., 2016) or whole cells (Braiek et al., 2012).

* Corresponding author.
*E-mail address:* Julian-David.Schrattenecker@ait.ac.at (J.D. Schrattenecker).

https://doi.org/10.1016/j.bios.2018.12.007

Available online 13 December 2018
0956-5663/ © 2018 Elsevier B.V. All rights reserved.

While EIS offers these highly attractive features, it suffers from several shortcomings and some researchers even concluded that it will be unlikely for EIS to become a reliable detection method for biomolecules (Vogt et al., 2016). The biggest issue is the stability of the sensor surface and thus the measured signal. Bogomolova et al. (2009) showed this instability issue with an EIS-sensor specific to thrombin (Bogomolova et al., 2009). In their experiments, $R_{CT}$ increased not only with the binding of the analyte but also by measuring multiple times. Other studies suspected that the commonly used redox-couple Hexacyanoferrat (II)/(III) (HCF) itself was the cause of these instabilities (Dijksma et al., 2002; Lazar et al., 2016). Lazar et al. (2016) thoroughly investigated the effect of HCF on gold electrodes. At concentrations of 1 mM HCF in PBS buffer, the $R_{CT}$ increased over a time period of about 200 min and then started to decrease. The resistance dropped until the measurement was stopped after 700 min, without reaching a steady value. Lazar et al. assumed that the HCF exchanges one of its ligands with a water molecule and releases cyanide. It is known, that cyanide solutions can dissolve gold (Syed, 2012). Dijksma et al. (2002) reported that even surface modifications, such a self-assembled monolayer (SAM), do not protect the gold surface. Over long periods of time the HCF corroded the gold surface and as a result the monolayer desorbed, which led to a decrease of the $R_{CT}$ (Dijksma et al., 2002). Although, the existing problems with the HCF were already documented, in a huge number of recent papers this potentially harmful substance was used in combination with gold electrodes, which may inhibit the performance of their sensors (Diaz-Cartagena et al., 2017; Lim et al., 2018; Shariati et al., 2018).

A convenient, alternative redox-probe has to fulfill a number of requirements to be suitable for EIS spectroscopy. These requirements include the stability of the oxidized and the reduced state. Furthermore, it must neither corrode the electrodes nor affect the functionalization on the electrodes nor interact with the analyte molecules. Substances that fulfill these requirements are scarce. Most substances, such as Hexaammineruthenium (III) ($[Ru(NH_3)_6]^{3+}$), are only stable in the oxidized state. To overcome this problem, a DC-bias is applied to the system to produce the reduced state Hexaammineruthenium (II) in-situ during the measurement in close vicinity to the working electrode. For this method, a three-electrode system is essential. EIS measurements with DC-bias have already been used with Hexaammineruthenium (III) as an alternative redox-probe to determine the impedances and the electron transfer through self-assembled monolayers by several researchers (Doubova et al., 2012; Ganesh et al., 2006; Mendez et al., 2008; Protsailo and Fawcett, 2000). However, until now, the Hexaammineruthenium (II)/(III) redox-pair has not been used in EIS-biosensors.

We introduced Hexaammineruthenium (II)/(III) produced by in-situ reduction of Hexaammineruthenium (III) as alternative redox-pair in EIS biosensors with gold electrodes to prevent corrosion and thus increase the stability of the measurement signal. First attempts to combine the in-situ production of the redox-pair with a fully functional biosensor have been made by us recently (Schrattenecker et al., 2017). In this work, we compared the stability of photolithographically fabricated thin-film (TF) and screen-printed (SP) gold electrodes in Hexacyanoferrate and Hexaammineruthenium solutions. Furthermore, we performed a long-time characterization of the electrochemical properties of these redox systems with cyclic voltammetry and electrochemical impedance spectroscopy.

We demonstrated the suitability of Hexaammineruthenium for biosensing by the impedimetric detection of human-IgG. Human IgG was chosen as biomarker because of its high diagnostic relevance for monitoring the overall health status. IgG is available in serum of a healthy person in concentrations of about 990 µg/mL (Furst, 2009). In saliva the concentration is approximately 60 times lower with about 16 µg/mL (Grönblad, 2009). The IgG levels can increase in cases of stress (Matos-Gomes et al., 2010) or during aerobic conditioning (Martins et al., 2009). A decrease of the IgG concentration in serum below 100 µg/mL increases the risk of infection tremendously (Furst, 2009). Therefore, a quantitative monitoring can be beneficial for athletes to prevent sickness and inhibition in their athletic performance at competitions.

## 2. Materials and methods

### 2.1. Chemicals and reagents

AffiniPure Goat Anti-Human IgG $F(ab)_2$-specific antibodies (109–005-006; IgG-Ab) were obtained from Jackson ImmunoResearch Europe Ltd (Newmarket, UK). 11-mercapto undecanoic acid 95% (MUA), 3-mercapto propionic acid 99% (MPA), N-(3-Dimethylaminopropyl)-N′-ethylcarbodiimide hydrochloride 99% (EDC), ethanolamine hydrochloride 99% (EA), N-Hydroxysulfosuccinimide sodium salt 98% (Sulfo-NHS), IgG from human serum with c = 4.87 mg/mL in buffered aqueous solution, 2-(N-morpholino)ethanesulfonic acid 99% (MES), Potassium hexacyanoferrat (II) trihydrat 99%, Dimethyl sulfoxide (DMSO) 99.9%, Potassium Hexacyanoferrat (III) 99% and Hexaammineruthenium (III) chloride 98% were obtained from Sigma-Aldrich (St. Louis, MO, USA). The negative photoresist maN 1440 and the developer ma-D 533/S were obtained from micro resist technology GmbH (Berlin, Germany). Other chemicals were of analytical quality and were used without further treatment.

### 2.2. Preparation of thin film sensors

Substrates for the electrodes were conventional glass microscope slides which were cleaned in a 5% aqueous detergent solution in an ultrasonic bath for 1 h. The substrates were then rinsed with ultrapure water and isopropyl alcohol, and were dried under a nitrogen stream. Prior to spin-coating, the slides were dried on a hot plate at 120 °C. Next, TI-Prime was spin-coated onto the slides (t = 20 s, 3000 rpm) using a Ramgraber spin-coater M-200 and heated to 120 °C for 1 min. Next, the negative photoresist was spin-coated onto the microscope slides (t = 20 s, 3000 rpm) and dried at 100 °C for 1 min. The slides with the photoresist were exposed to UV light with an energy of about 300 mJ/cm$^2$ in the EVG 620 mask aligner from EVG (St. Florian am Inn, UA, Austria) using an appropriate lithography mask. The UV light exposed slides were developed for 4 min, rinsed twice with ultrapure water and dried in a nitrogen gas stream at room temperature.

To remove photoresist residues on the glass surface, the slides were treated with oxygen plasma (room temperature, 5 min, 1 mbar, 60 W) using the plasma cleaner Femto from Diener electronic GmbH + Co. KG (www.plasma.de) prior to the deposition of the metallic layers. After the plasma ashing about 5 nm chromium and 200 nm gold were deposited by physical vapor deposition (PVD). Lift-off was done in DMSO at 70 °C for several hours. Next, the slides were cleaned by ultrasonication followed by two times rinsing with isopropyl alcohol and drying under nitrogen gas flow. Before the functionalization, the sensors were cleaned with piranha solution ($H_2SO_4$:$H_2O_2$ = 3:1) for 10 min. After the cleaning the sensors were washed with de-ionized water.

### 2.3. Preparation of screen-printed sensors

Screen-printed (SP) sensors from BVT Technologies (www.bvt.cz) of the type AC1. W1.R2 with a three-electrode setup, consisting of a AgCl covered Ag reference electrode, a gold working electrode and a gold counter electrode, screen-printed on a ceramic substrate, were used. The sensors were cleaned in water and ethanol for 10 min by ultrasonication. The surface was further cleaned electrochemically in 50 mM $H_2SO_4$ by applying a constant voltage of 1.4 V (vs Ag/AgCl reference electrode) for 25 s. After the electrochemical cleaning, the sensors were washed with water.

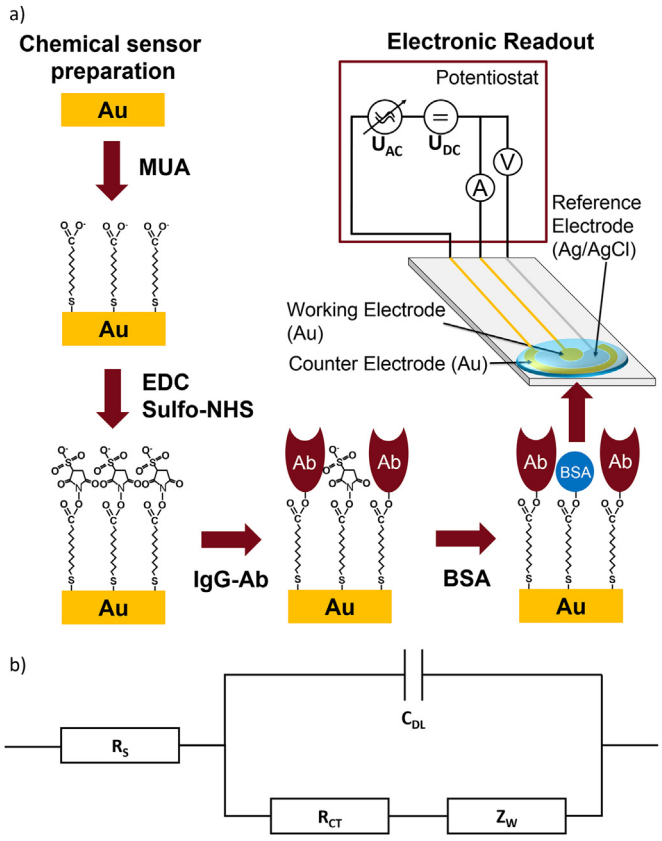


**Fig. 1.** a) Schematic of the sensor functionalization and the electronic readout; b) Randles circuit used for curve fitting.

### 2.4. Biosensor preparation

A 10 mM MUA solution in a mixture of 95% ethanol and 5% de-ionized water was applied for about 16 h to form the monolayer. In case of the sensors with MPA layer, a 10 mM MPA solution in de-ionized water was used. In a next step, the sensors were washed with ethanol and de-ionized water. Subsequently, the carboxylic acid groups were activated with a 25 mM EDC and 25 mM Sulfo-NHS solution in 60 mM MES buffer solution with pH 4.7 for 1 h. Then, the sensors were washed again with de-ionized water and incubated with 90 µL $F(ab)_2$-specific IgG-Ab solution (c = 240 µg/mL IgG-Ab in PBS) for 2 h. Finally, the sensors were washed with a 0.1 mg/mL BSA solution and incubated for 1 h in about 100 µL of this solution to block the remaining activated carboxylic acid groups. Fig. 1a shows a schematic of the functionalization steps.

### 2.5. CV measurement method

The cyclic voltammetry (CV) measurements were performed in 10 mM PBS buffer at pH 7.4 with an Autolab potentiostat PGSTAT30 (www.metrohm-autolab.com). The applied voltage ranges were − 0.5 to 0 V for the screen-printed electrodes with 10 mM Hexaammineruthenium (III) chloride as redox-probe, and − 0.15 to 0.4 V with 5 mM HCF as redox-probe. The scan rate was 100 mV/s and the step potential resolution of the set value was 2.44 mV. All of the mentioned potentials refer to the integrated Ag/AgCl reference electrode placed in the measurement solution otherwise noted.

### 2.6. EIS measurement method

For the electrochemical impedance spectroscopy measurements the Autolab potentiostat PGSTAT30 with the FRA2 module was used for impedance analysis. The measurement solution consisted of 10 mM Hexaammineruthenium (III) chloride in 10 mM PBS buffer at pH 7.4. For the stability measurements, a 5 mM HCF solution in 10 mM PBS buffer at pH 7.4 was used. The measurements with Hexaammineruthenium (III) were performed with a DC-bias of − 160 mV to reduce Hexaammineruthenium (III) to Hexaammineruthenium (II) at the working electrode. Additionally to the DC-bias, an AC signal with a peak amplitude of 5 mV was applied to the screen-printed electrodes, as schematically depicted in Fig. 1a. In case of the thin-film (TF) sensors, no DC-bias was applied during the EIS measurements. The measured frequencies ranged from 120 kHz to 1 Hz. The curve fitting using the Randles circuit (see Fig. 1b) was performed directly in the NOVA 2.0 measurement software from Metrohm Autolab B.V. (Utrecht, The Netherlands) and in Matlab (Natick, MA, USA). Constant phase elements (CPE) were used during the curve fitting to describe the double layer capacitance and the Warburg impedance respectively.

## 3. Results and discussion

### 3.1. Study of sensor stability with HCF as redox-probe

#### 3.1.1. Thin-film sensors with two-electrode system

To determine the stability of differently functionalized thin-film sensors, the EIS spectra were recorded over time with 5 mM HCF as redox-probe. Fig. 2a depicts the recorded EIS spectra of a thin-film sensor functionalized with Au/MPA/IgG-Ab/BSA. Even after 60 min of measurement time, the recorded spectra differed significantly and kept changing. In more detail, the variation of the charge transfer resistance within this one hour, which is the key parameter for a working EIS biosensor, is depicted in Fig. 2c. The EIS spectrum was recorded every two minutes over a time frame of 60 min, which corresponds to 31 measurement points. $R_{CT}$ shows a quite drastic change with a mean value of about 120% of the starting value. During the measurements even values up to about 140% have been recorded. This signal change, which occurs already after a few minutes, can be attributed to the ability of HCF to corrode the gold electrodes. Over longer incubation times, the influence of the HCF on the gold electrodes is much more drastic, as it is illustrated in Fig. 3. Fig. 3a depicts a freshly prepared and cleaned thin-film sensor with gold electrodes. This sensor was incubated with 5 mM HCF in 10 mM PBS buffer at pH 7.4 for 7 days. After this incubation nearly all of the gold was dissolved and the chromium adhesion layer became visible (see Fig. 3b). Even short measurement times can influence the measurement stability and can lead to an early destruction of the functionalization rendering the biosensor useless. The application of a thicker monolayer to protect the gold electrodes also did not lead to a more stable measurement system. A thin-film sensor with MUA/IgG-Ab/BSA functionalization was used for EIS measurements with 5 mM HCF in PBS as redox-probe. The recorded EIS spectra, shown in Fig. 2b, were not stable, even over longer measurement times. Therefore, it can be concluded that the increase of the chain length of the monolayer from three carbon atoms to eleven carbon atoms does not increase the stability of the gold electrodes at all.

#### 3.1.2. Screen-printed sensors with three-electrode system

The stability of the screen-printed three-electrode system with MUA/IgG-Ab/BSA functionalization against HCF was tested with CV and EIS. The CV curves were recorded every minute. As Fig. 4a shows, the CV measurements with HCF as redox-probe drifted to higher currents over the whole measurement time and even after 70 min of measurement the drift did not stop. The increase of the current can be attributed to the corrosion of the gold electrodes and the associated removal of the functionalization. The EIS spectra were also recorded for this type of sensor with a DC-bias of 140 mV, which corresponds to the potential of the redox couple HCF. The EIS spectra in Fig. 4b show that the recorded signals did not remain stable and behaved similarly to the

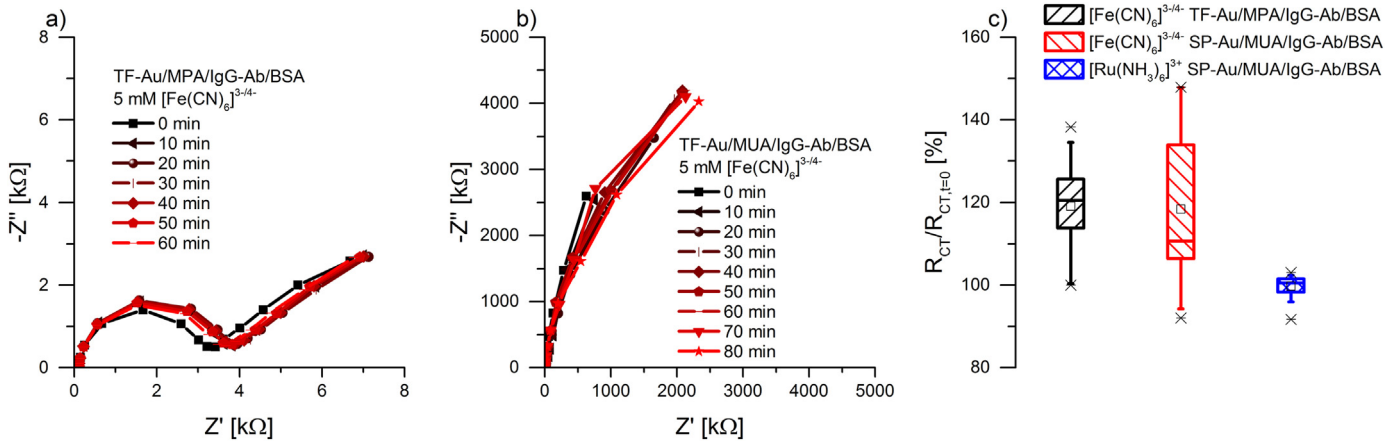


**Fig. 2.** a) EIS spectra over time of a MPA/IgG-Ab/BSA functionalized thin-film sensor with 5 mM HCF as redox-probe; b) EIS spectra over time of a MUA/IgG-Ab/BSA functionalized thin-film sensor with 5 mM HCF as redox-probe; c) Box plot for stability of biosensors over long measurement times of a MPA/IgG-Ab/BSA functionalized thin-film sensor (black) and a MUA/IgG-Ab/BSA functionalized screen-printed sensor (dark red) with 5 mM HCF in PBS as redox-probe, and a MUA/IgG-Ab/BSA functionalized screen-printed sensor with 10 mM $[Ru(NH_3)_6]^{3+}$ in PBS as redox-probe (blue); each sensor was measured every two minutes over a period of 60 min, number of measurements m = 31. (For interpretation of the references to color in this figure legend, the reader is referred to the web version of this article).

thin-film sensors. The charge transfer resistance kept changing over 60 min and did not reach a stable value. Fig. 2c depicts this variation of the $R_{CT}$ over time as red box plot. The $R_{CT}$ value kept changing throughout the measurement. It varied from nearly 150% to about 90% of the starting value. Neither the different monolayers nor the different production technique of the gold electrode positively influenced the stability of the sensor against HCF.

### *3.2. Study of sensor stability with Hexaammineruthenium (III) as redox-probe*

As a solution to the above described stability problem of EIS sensors with gold electrodes employing HCF, we investigated Hexaammineruthenium (III) as redox-probe. We used the previously mentioned screen-printed three-electrode sensors and a CV was

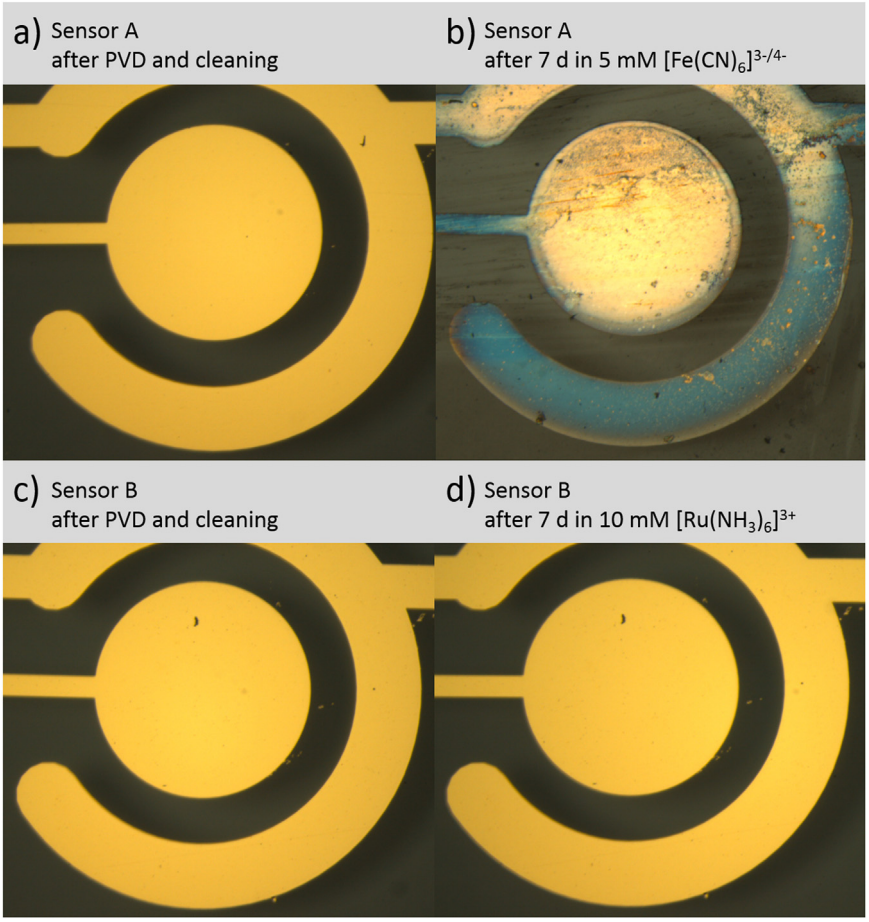


**Fig. 3.** a) Sensor A, new thin-film sensor after PVD and cleaning; b) Sensor A after 7 days of incubation in PBS with 5 mM HCF; c) Sensor B, new TF sensor after PVD and cleaning; d) Sensor B after 7 days of incubation in PBS with 10 mM Hexaammineruthenium (III).

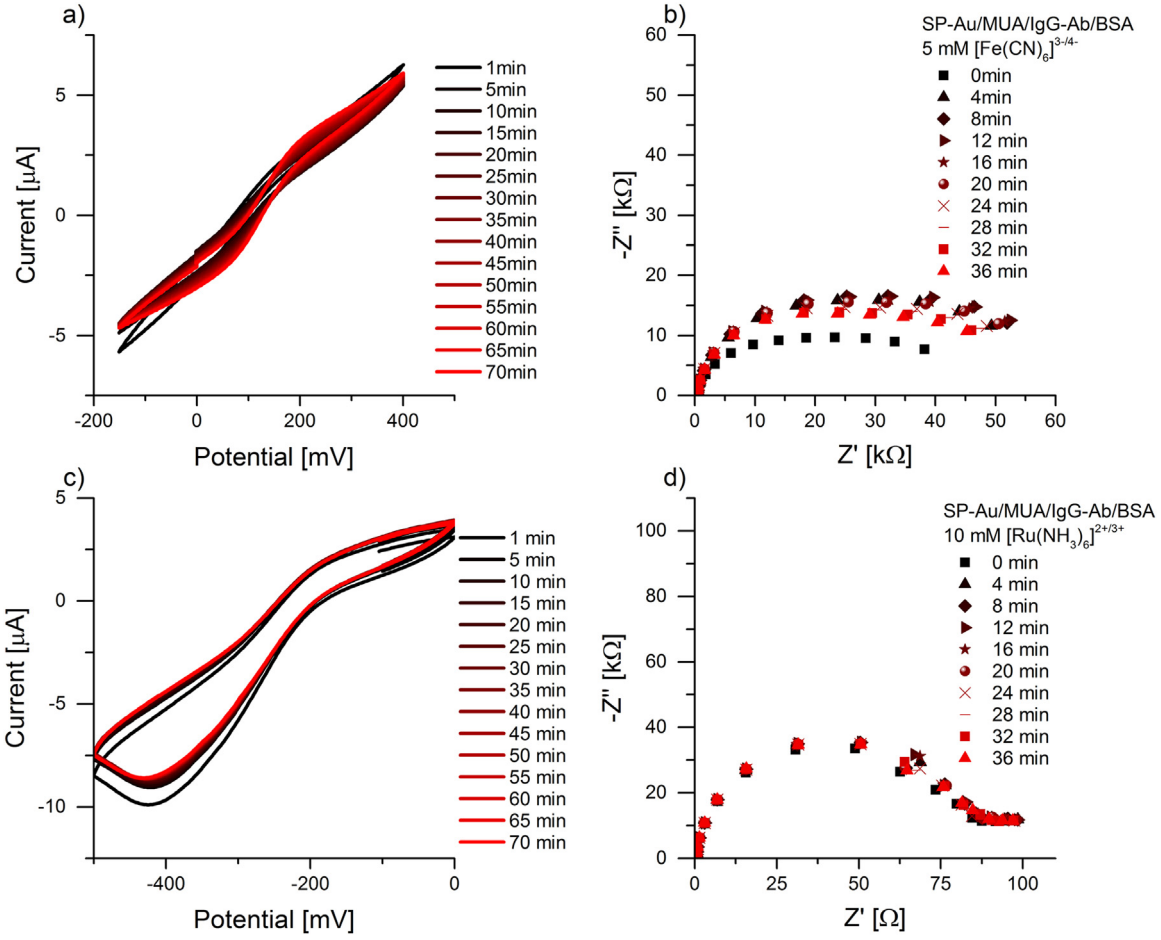


**Fig. 4.** a) CV over time of a MUA/IgG-Ab/BSA functionalized screen-printed sensor with 5 mM HCF as redox-probe; b) EIS spectra of a MUA/IgG-Ab/BSA functionalized screen-printed sensor with 5 mM HCF as redox-probe and a DC-bias 0.14 V; c) CV over time of a MUA/IgG-Ab/BSA functionalized screen-printed sensor with 10 mM Hexaammineruthenium (III) as redox-probe; d) EIS spectra of a MUA/IgG-Ab/BSA functionalized screen-printed sensor with 10 mM Hexaammineruthenium (III) as redox-probe and a DC-bias − 0.16 V. (For interpretation of the references to color in this figure, the reader is referred to the web version of this article).

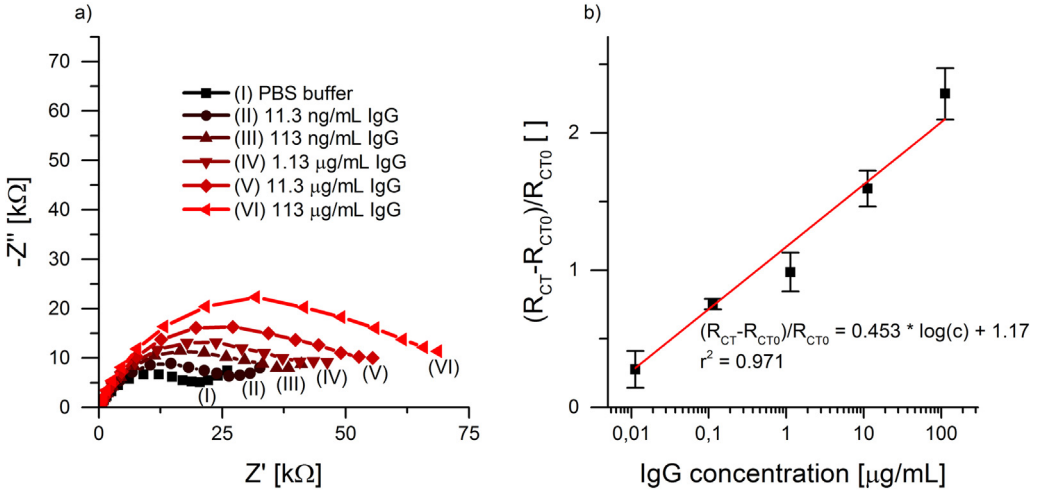


**Fig. 5.** a) Nyquist plots of a screen-printed biosensors with MUA/IgG-Ab/BSA functionalization after 30 min of incubation in (I) PBS, (II) 11.3 ng/mL IgG, (III) 113 ng/mL IgG, (IV) 1.13 µg/mL IgG, (V) 11.3 µg/mL IgG, and (VI) 113 µg/mL IgG; b) calibration curve of buffered IgG solutions with relative $R_{CT}$ versus IgG concentration in half-logarithmic form, number of measurements m = 3.

performed every minute. Fig. 4c shows the CV curves for a screen-printed three-electrode sensor with an MUA/IgG-Ab/BSA functionalization. The curves clearly reached a stable signal after the first few measurements and remained stable even after 70 min. The EIS measurements were performed every two minutes with a DC-bias of − 160 mV to reduce Hexaammineruthenium (III) to Hexaammineruthenium (II) in-situ during the impedance measurements. This DC-bias was chosen because it is close to the DC-bias at which the oxidized state and reduced state are available in the same concentration on unfunctionalized gold electrodes. The EIS spectra depicted in Fig. 4d indicate that the impedances changed marginally after the initial measurement and stayed stable even after 36 min. The

**Table 1**
$R_{CT}$, relative $R_{CT}$, and corresponding standard deviation of buffered IgG solutions for concentrations ranging from 11.3 ng/mL to 113 µg/mL.

| Concentration [µg/mL IgG] | Average $R_{CT}$ [kΩ] | $(R_{CT}-R_{CT0})/R_{CT0}$ | Standard deviation |
|---|---|---|---|
| 0.0113 | 26.2 | 0.3 | 0.1 |
| 0.113 | 36.0 | 0.75 | 0.04 |
| 1.13 | 40.8 | 1.0 | 0.1 |
| 11.3 | 53.3 | 1.6 | 0.1 |
| 113 | 67.5 | 2.3 | 0.2 |

charge transfer resistance remained stable for nearly 60 min with only little change, as shown in Fig. 2c in the blue box plot. The lowest recorded $R_{CT}$ was 90% and the highest 100% of the starting value. As the CV and the EIS measurements show, the stability of the measured signals was increased significantly. The influence of Hexaammineruthenium (III) over several days, as previously shown with HCF, was also tested. Fig. 3c depicts a newly prepared sensor after PVD and cleaning. This sensor was incubated in PBS with 10 mM Hexaammineruthenium (III) for seven days. The electrodes showed no visual change after this period of time (see Fig. 3d). When a thin-film sensor was incubated for the same time period in HCF, the gold removed in large amounts and the chromium layer underneath the gold becomes visible, as depicted in Fig. 3b.

### 3.3. EIS response to IgG-binding

The functionalized biosensor was incubated for 30 min in a PBS buffer solution and the EIS spectrum was recorded as a baseline, shown as black curve in Fig. 5a. In subsequent steps, the biosensor was incubated with buffered IgG solutions with increasing concentrations ranging from 11.3 ng/mL to 113 µg/mL and the respective impedances were recorded. During these incubation steps, the human IgG was bound to the $F(ab)_2$-specific-human-IgG antibody by protein-protein interaction. This binding of the analyte lead to an increase of $R_{CT}$ and $C_{DL}$. Fig. 5a visualizes the increase of the impedance in dependence of the human-IgG concentration. After incubation with the lowest concentration of 11.3 ng/mL the $R_{CT}$ already increased to 26.2 kΩ. With higher concentrations of IgG the charge transfer resistance $R_{CT}$ rose further, until it reached 67.5 kΩ at 113 µg/mL, as summarized in Table 1.

The obtained charge transfer resistance values were used to calculate a relative resistance change by subtracting the $R_{CT}$ value of the blind control $R_{CT0}$ and then dividing by this value to suppress the influence of variations in the functionalization procedure. The relative resistance versus the logarithmic human-IgG concentration showed a linear response (see Fig. 5b). The calibration curve had a sensitivity of 0.453 per decade and a linear correlation coefficient of 0.971. This linear response was present over a wide range of five decades of concentration. At the highest concentration the standard deviation was about 0.2.

## 4. Conclusion

In this work, we have successfully introduced Hexaammineruthenium (III) as an alternative redox-probe to replace HCF in electrochemical impedance spectroscopy for the detection of biomolecules using gold electrodes. By applying a DC-bias during the EIS measurement we generated Hexaammineruthenium (II)/(III). The redox pair Hexaammineruthenium (II)/(III) did not cause a degradation of the gold electrodes, and thus, allowed recording stable EIS signals for at least 60 min. This is a prerequisite for high precision and reliable EIS measurements. The $R_{CT}$ value decreased only by 10%, in comparison to a variation between 100% and 140% when HCF was used as redox-pair measuring a constant analyte concentration. Neither the production method, i.e. screen-printing or thin-film process, nor the surface coverage of the sensor, either MUA or MPA monolayer, resulted in sufficiently stable gold electrodes for EIS measurements with HCF as redox-probe. In contrast, the use of the in-situ generated Hexaammineruthenium (III) redox-probe improved the stability of the sensor significantly and reduced the risk of false sensor signals. Furthermore, Hexaammineruthenium (III) was applied as redox-probe to realize a human-IgG biosensor based on EIS. The measured signals were stable and the sensor showed a good linear correlation of 0.971 to the logarithm of IgG-concentrations over five decades, ranging from 11.3 ng/mL to 113 µg/mL IgG.

In summary, our approach overcomes the current shortcomings of EIS associated with HCF, which paves the way to employ the EIS technique as reliable biosensing method for point-of-care-testing applications. We expect that additional optimization of the functionalization and the DC-bias can improve the sensor performance even further. An important next step will be the application of Hexaammineruthenium for EIS biosensing in biological samples such as serum and saliva.

## Acknowledgement

This study was supported by Infineon Technologies Austria AG.

## References

Arya, S.K., Chornokur, G., Venugopal, M., Bhansali, S., 2010. Biosens. Bioelectron. 25 (10), 2296–2301.
Bahadır, E.B., Sezgintürk, M.K., 2016. Artificial cells. Nanomed. Biotechnol. 44 (1), 248–262.
Bănică, F.-G., 2012. Chemical Sensors and Biosensors. John Wiley & Sons, Ltd, Chichester, UK.
Bogomolova, A., Komarova, E., Reber, K., Gerasimov, T., Yavuz, O., Bhatt, S., Aldissi, M., 2009. Anal. Chem. 81 (10), 3944–3949.
Braiek, M., Rokbani, K., Chrouda, A., Mrabet, B., Bakhrouf, A., Maaref, A., Jaffrezic-Renault, N., 2012. Biosensors 2 (4), 417–426.
Diaz-Cartagena, D.C., Hernández, G., Bracho-Rincon, D., González-Feliciano, J.A., Cunci Perez, L., González, C.I., Cabrera, C.R., 2017. ECS Trans. 77 (11), 1833–1840.
Dijksma, M., Boukamp, B.A., Kamp, B., van Bennekom, W.P., 2002. Langmuir 18 (8), 3105–3112.
Doubova, L.M., Fabrizio, M., Daolio, S., Forlini, A., Rondinini, S., Vertova, A., 2012. Russ. J. Electrochem. 48 (4), 351–363.
El Harrad, L., Bourais, I., Mohammadi, H., Amine, A. 2018. Sensors. Basel, Switzerland, 18, 1.
Furst, D.E., 2009. Semin. Arthritis Rheum. 39 (1), 18–29.
Ganesh, V., Pal, S.K., Kumar, S., Lakshminarayanan, V., 2006. J. Colloid Interface Sci. 296 (1), 195–203.
Grönblad, E.A., 2009. Acta Odontol. Scand. 40 (2), 87–95.
Huang, Y., Xu, J., Liu, J., Wang, X., Chen, B., 2017. Sensors. Basel, Switzerland, 17, 10.
Lazar, J., Schnelting, C., Slavcheva, E., Schnakenberg, U., 2016. Anal. Chem. 88 (1), 682–687.
Lim, J.M., Kim, J.H., Ryu, M.Y., Cho, C.H., Park, T.J., Park, J.P., 2018. Anal. Chim. Acta 1026, 109–116.
Martins, R.A., Cunha, M.R., Neves, A.P., Martins, M., Teixeira-Veríssimo, M., Teixeira, A.M., 2009. Int. J. Sports Med. 30 (12), 906–912.
Matos-Gomes, N., Katsurayama, M., Makimoto, F.H., Santana, L.L.O., Paredes-Garcia, E., Becker, M.Ad, Dos-Santos, M.C., 2010. Neuroimmunomodulation 17 (6), 396–404.
Mendez, E., Worner, M., Lages, C., Cerda, M.F., 2008. Langmuir: ACS J. Surf. Colloids 24 (9), 5146–5154.
Mills, D.M., Martin, C.P., Armas, S.M., Calvo-Marzal, P., Kolpashchikov, D.M., Chumbimuni-Torres, K.Y., 2018. Biosens. Bioelectron. 109, 35–42.
Montes, R., Céspedes, F., Baeza, M., 2016. Biosens. Bioelectron. 78, 505–512.
Moon, J.-M., Thapliyal, N., Hussain, K.K., Goyal, R.N., Shim, Y.-B., 2018. Biosens. Bioelectron. 102, 540–552.
Protsailo, L.V., Fawcett, W., 2000. Electrochim. Acta 45 (21), 3497–3505.
Randviir, E.P., Banks, C.E., 2013. Anal. Methods 5 (5), 1098.
Schrattenecker, J.D., Heer, R., Hainberger, R., Fafilek, G., 2017. Proceedings 1 (3), 534.
Shariati, M., Ghorbani, M., Sasanpour, P., Karimizefreh, A., 2018. Anal. Chim. Acta.
Syed, S., 2012. Hydrometallurgy 115–116, 30–51.
Vogt, S., Su, Q., Gutierrez-Sanchez, C., Noll, G., 2016. Anal. Chem. 88 (8), 4383–4390.